



Evaluation of DC wind turbine concepts for coupling wind energy with electrolysis

Florian Andresen¹ · Fabian Herzog¹ · Benedict J. Mortimer¹ · Rik W. De Doncker¹

Received: 15 September 2024 / Accepted: 30 January 2025
© The Author(s) 2025

Abstract

Increasing energy generation from renewable energy sources results in a larger number of power electronic converters and filters, which introduce additional cost, losses and downtimes due to failures. Furthermore, hydrogen is becoming increasingly relevant as an energy carrier, both for storing energy and for decarbonizing industry production. Since wind turbine converters and electrolyzers operate internally with dc voltage, dc collector grids have become a promising solution with lesser conversion stages and simple integration of electrolyzer systems. First, this paper introduces three wind turbine configurations for energy collection by dc grids: A full-scale converter concept, a partial-scale converter concept and a novel concept based on the galvanically isolated three-phase dual active bridge. The wind turbine concepts are evaluated for their feasibility in a wind energy system connected to an electrolysis plant based on dc technology. Each concept is analyzed for its electrical characteristics, torque ripple, efficiency and investment cost. In contrast to a traditional ac system, the number of conversion stages and filters is reduced while coupling with other dc-based technologies like photovoltaic or batteries.

Bewertung von DC-Windturbinenkonzepten zur Kopplung von Windenergie und Elektrolyse

Zusammenfassung

Die zunehmende Energieerzeugung aus erneuerbaren Energiequellen führt zu einer größeren Anzahl von leistungselektronischen Umrichtern und Filtern, die zusätzliche Kosten, Verluste und Ausfallzeiten aufgrund von Ausfällen verursachen. Darüber hinaus gewinnt Wasserstoff als Energieträger zunehmend an Bedeutung, sowohl für die Speicherung von Energie als auch für die Dekarbonisierung der Industrieproduktion. Da Windturbinenumrichter und Elektrolyseure intern mit Gleichspannung arbeiten, sind Gleichstromnetze eine vielversprechende Lösung mit weniger Umwandlungsstufen und einfacher Integration von Elektrolyseursystemen. In dieser Arbeit werden zunächst drei DC-Windturbinenkonzepte vorgestellt: Ein Vollumrichterkonzept, ein Teilumrichterkonzept und ein neuartiges Konzept, das auf einer galvanisch getrennten dreiphasigen Dual-Active Bridge basiert. Die Windturbinenkonzepte werden hinsichtlich ihrer Eignung für eine Windkraftanlage bewertet, die über ein Gleichstromnetz mit einer Elektrolyseanlage verbunden ist. Jedes Konzept wird auf seine elektrischen Eigenschaften, die Drehmomentwelligkeit, den Wirkungsgrad und die Investitionskosten hin untersucht. Im Gegensatz zu einem traditionellen Wechselstromsystem wird die Anzahl der Umwandlungsstufen und Filter bei der Kopplung mit anderen gleichstrombasierten Technologien wie Photovoltaik oder Batterien reduziert.

1 Introduction

Generating electrical energy from renewable energy sources (RES) like wind and solar has become increasingly dominant as the world's energy supply shifts away from fossil fuels. Hydrogen, categorized as gray, blue, or green based on its production method, varies significantly in carbon emissions: gray hydrogen, produced from natural gas without mitigation, releases substantial CO₂; blue hydrogen incor-

✉ Florian Andresen
florian.andresen@eonerc.rwth-aachen.de

Rik W. De Doncker
post_pgs@eonerc.rwth-aachen.de

¹ Institute for Power Generation and Storage Systems, RWTH Aachen University, Aachen, Germany

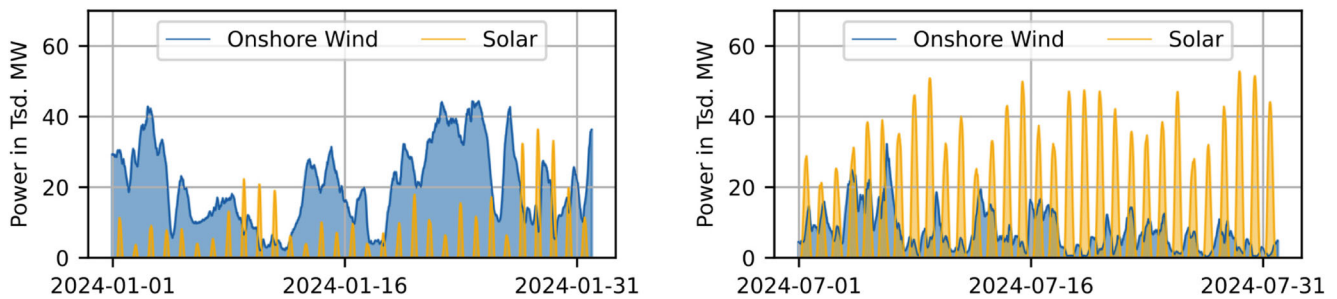


Fig. 1 Power generation in Germany by onshore wind and solar power in January 2024 and July 2024 [4]

porates carbon capture to reduce emissions; and green hydrogen, derived via electrolysis using renewable energy, is carbon-free. Hence, green hydrogen has become an attractive energy carrier for decarbonization of energy-intensive sectors as heavy industry and large-scale transportation [1].

The economic efficiency of electrolyzers heavily depends on the annual operating time [2]. The higher the full load hours of a system, the more worthwhile the investments become, as more hydrogen can be produced. At the same time, electricity costs need to be low in order to achieve a competitive hydrogen price. To decouple from electricity prices and take advantage of the drastic reductions in the levelized cost of electricity from wind energy in recent years, the direct coupling of generation plants and electrolyzers seems reasonable. The economic feasibility then depends on the number of full load hours that the renewable generation plants can produce annually at the specific location. In Germany, onshore wind turbines can achieve 1800h on the mainland, 2500h in northern Germany and 3000h near the coast [3]. However, the annual full load hours of the electrolyzer can be increased by combining wind and solar energy. This becomes apparent in Fig. 1, which shows the power generation in Germany by onshore wind and solar power in January 2024 and July 2024: In the winter months, energy generation from wind power typically dominates, while solar power is more relevant in the summer months. Furthermore, storage systems

like batteries can reduce power fluctuations and provide a more constant input power flow to the electrolyzer.

Given that wind turbine (WT) s, photovoltaic systems and electrolyzers operate internally on direct-current (dc) or use internal dc-links it is reasonable to utilize dc technology for coupling power generation and hydrogen production. Cost savings on investments and efficiency improvements, compared with traditional alternating-current (ac) solutions, are achieved due to a reduced number of conversion stages, smaller filter size, and reduced cable losses, as shown in a study on dc collector grids for offshore wind farms [5].

A key component for the application of dc technology in WTs is a high-power dc-dc converter, which meets various requirements such as stepping up/down dc voltages, galvanic isolation and fault ride-through capability. Firstly introduced in [6], the three-phase dual-active bridge (DAB3) has proven to be a feasible solution because of its inherent soft-switching capability, bidirectional powerflow, wide operation range and reduced filter size [7, 8]. Figure 2 shows the schematic of a DAB3 which consists of two three-phase half-bridges coupled via a medium-frequency transformer.

This work is structured as follows: Sect. 2 compares coupling of wind energy and electrolysis via ac-technology to coupling via dc-technology. Then, section Sect. 3 introduces three different dc-WT configurations and outlines advantages and disadvantages. Finally, in Sect. 4 an

Fig. 2 Schematic of a DAB3

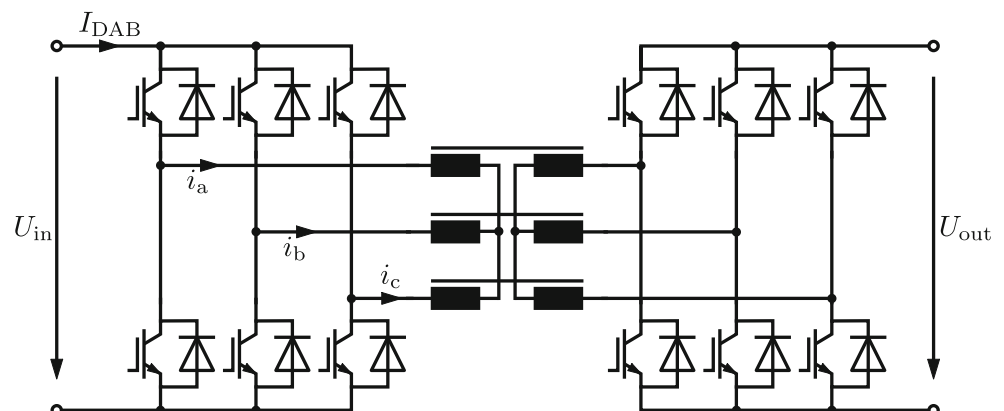
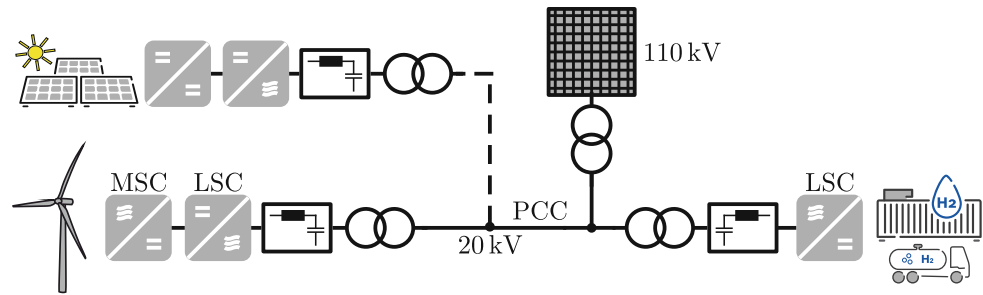


Fig. 3 Coupling of wind energy and electrolysis via ac

economic evaluation is done for all dc-WT configurations in comparison to existing ac configurations.

2 Coupling wind energy and electrolysis

This section presents the two main concepts of coupling an onshore WT to a hydrogen production plant. The necessary components and converter stages to realize coupling via an ac or dc connection are presented.

2.1 Coupling via AC

A typical grid connected WT, as shown in Fig. 3, consists of a machine-side converter (MSC), which does maximum power-point tracking (MPPT). Subsequently, the line-side converter (LSC) feeds active and reactive power into the grid. A filter reduces harmonic components caused by switching actions of the converter. Finally, a step-up transformer increases the voltage-level and a medium-voltage cable transfers power to the point of common coupling (PCC).

In this concept, the electrolyzer is connected to this internal medium-voltage grid at the PCC. Again, a transformer steps down the voltage and a power electronic converter rectifies the ac voltage and feeds the electrolyzer with the required current. Additionally installed solar power plants and a connection to the public grid enable generation of hy-

drogen in case of reduced power output from the WT and increase the amount of annual full load hours. For ac grid connection, the solar power plant requires an LSC, filter and a step-up transformer. However, this increases the investment cost and energy losses which makes the hydrogen production costs more dependent on volatile energy prices because the energy losses have to be compensated from the grid.

2.2 Coupling via DC

Coupling of wind energy and electrolysis via dc reduces the number of conversion stages. The LSC, rectifier of the electrolyzer and their grid filters are omitted, while the transformers get replaced by a DAB3. Figure 4 shows the exemplary configuration. A common dc bus with a nominal voltage of $U_{dc} = 5$ kV is considered and realized as a bipolar dc bus, as it reduces line-to-ground insulation efforts.

The advantages of the dc concept become even more visible when the integration of solar power is taken into account. Here, LSC, filter and step-up transformer can be omitted as well. Combined power generation from wind and solar power and a higher efficiency due to lesser conversion stages could increase annual full-time hours of the electrolyzer. Consequently, the demand for electricity from the grid is reduced.

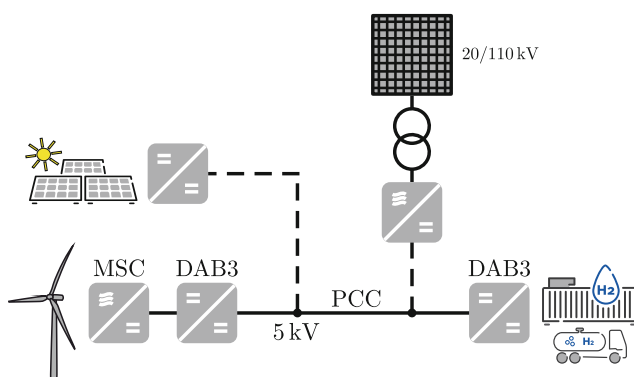
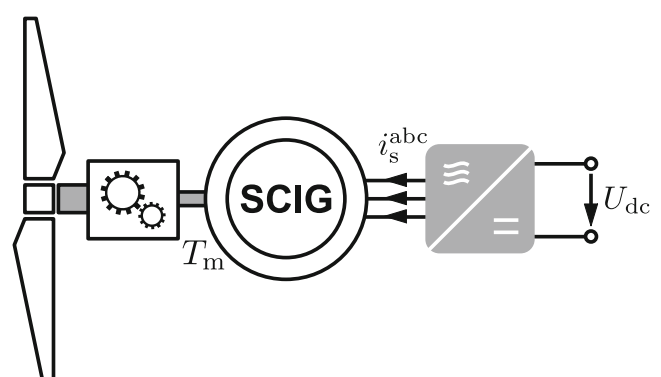
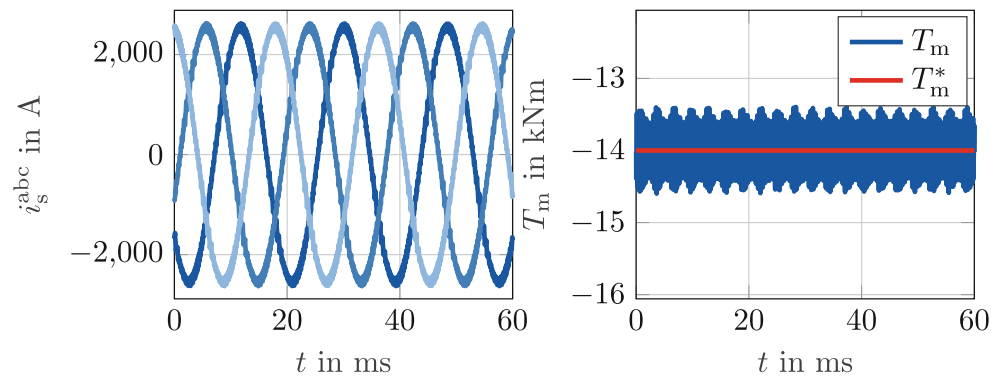
**Fig. 4** Coupling of wind energy and electrolysis via dc**Fig. 5** Full-scale converter concept for a dc-WT

Fig. 6 PLECS simulation of DC-SCIG showing stator currents and torque



3 DC wind turbine concepts

A key component to maximize the full potential of the dc-concept is a dc-WT that can be directly connected to a dc-grid. There are several electrical drivetrain concepts which enable the variable-speed operation of dc grid-connected WTs. Similar to ac grid connected WTs and dependent on the type of generator and the power electronic converter topology, most of them can be divided into full-scale and partial-scale concepts [5]. Additionally, a novel concept utilizing a DAB3 is introduced. Basic control concepts were developed to validate the functionality of the individual concepts which will not be discussed in detail here.

3.1 Full-scale converter concept

Full-scale converter concepts are characterized by a converter which is designed to transfer the entire generated power. In ac-connected WTs, a full-scale converter consists typically of two back-to-back connected converters: an MSC and an LSC. Hereby, the MSC controls torque and flux in the generator; the LSC the internal dc-link voltage and reactive power which is fed into the grid. As can be seen in Fig. 5, a dc grid-connected full-scale WT does not require an LSC with a corresponding grid filter. The MSC is realized depending on the rated line-to-line voltage of the generator $U_{LL,WT}$. A 2-level active front end (2L-AFE) is suitable for $U_{LL,WT} = 690$ V and a 3-level neutral-point clamped 3L-NPC converter [9] can be used for medium-voltage generators in offshore applications with $U_{LL,WT} = 3.3$ kV and a rated power of more than 10 MW. It is possible to realize the generator using either an squirrel-cage induction generator (SCIG) or a permanent-magnet synchronous generator (PMSG).

Figure 6 shows the results of a PLECS simulation of a DC-SCIG. Hereby, an SCIG with a nominal power of $P_{SCIG} = 2.75$ MW and rated line-to-line voltage $U_{LL,WT} = 690$ V is turning at nominal speed. And the MSC operating with a switching frequency of $f_{sw} = 2.5$ kHz and dc link voltage $U_{dc} = 1100$ V, controls the torque to a constant

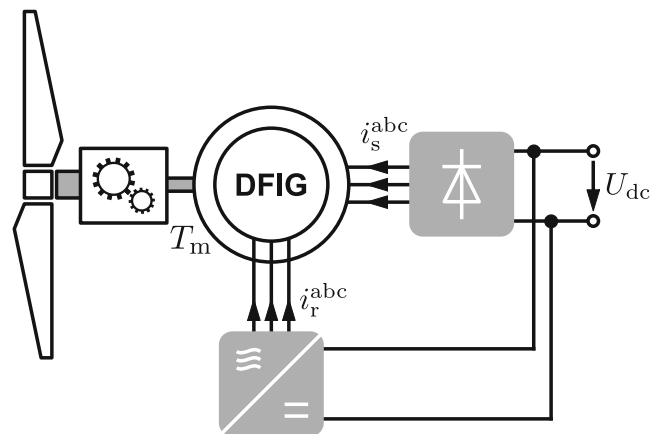


Fig. 7 Partial-scale converter concept for a dc-WT

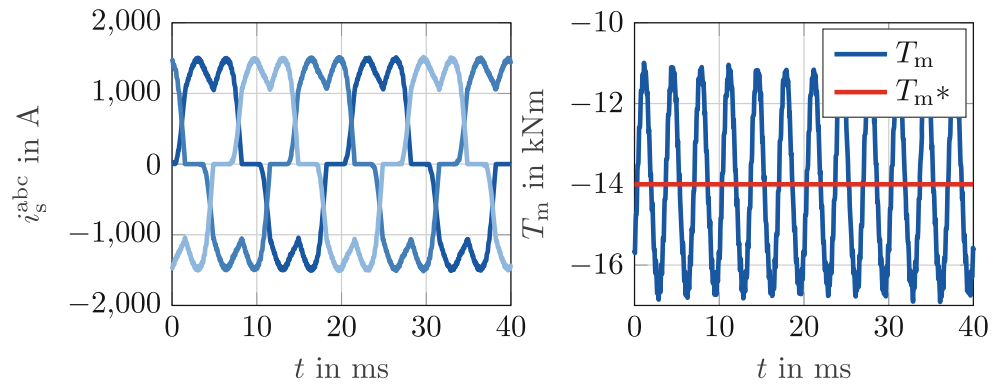
reference value T_m^* . It can be seen that, the DC-SCIG is able to produce almost sinusoidal currents resulting in constant torque with low torque ripple.

On the one hand this concept requires a high power electronic effort, but on the other hand this approach offers the most flexibility regarding the variability of wind speed, well-known control methods can be adopted from ac grid connected WTs and the low ripple minimizes possible effects on the mechanical drivetrain.

3.2 Partial-scale converter concept

In partial-scale concepts, the converter is rated for only a fraction of the WT system. Similar to full-scale converter concepts, the electrical drivetrain of the ac grid-connected partial-scale converter concept consists of a doubly-fed induction generator (DFIG) with an MSC and an LSC with corresponding grid filter. The power electronic components are typically rated to about 30% of the WT system which leads to speed variability of the same amount around the nominal speed [10]. Figure 7 shows a partial-scale WT system which is connected to a dc grid. An LSC and filter are not required. The MSC is connected to the rotor via slip rings and controls stator frequency and torque of the

Fig. 8 Plescs simulation of DC-DFIG showing stator currents and torque



generator. A passive three-phase diode rectifier enables connection of the stator to the dc grid. The operation principle of this concept has already been demonstrated on a small-scale [11].

This concept offers lower investment cost of power electronic components because of reduced converter rating and utilization of inexpensive and robust diodes for rectification. The diode rectifier offers a higher efficiency because of less switching actions in comparison to an active rectifier. The losses in the MSC are reduced as well because it only transfers a fraction of the WT's rated power. Control methods for the MSC can be adopted partly from ac-connected WT's and there is an additional degree of freedom because the stator frequency is not fixed to the grid

frequency anymore. However, it is possible that the non-linear characteristics of the diode rectifier cause additional stress to the mechanical drivetrain, due to increased torque harmonics. This becomes visible in the PLECS simulation results shown in Fig. 8. The simulation was done using the same parameters for generator and MSC as in the previous section. First, the stator currents contain a high amount of harmonics. Especially the 5th multiple of the fundamental frequency component causes a significant current distortion. This results in a large amount of torque ripple at the 6th multiple of the stator frequency because the torque is controlled in a stator-flux oriented reference frame. Different control approaches have been presented in order to mitigate this problem [12, 13]. However, the effects on the mechan-

Fig. 9 A dc-WT concept, consisting of a PMSG, connected to a DAB3 via a diode rectifier

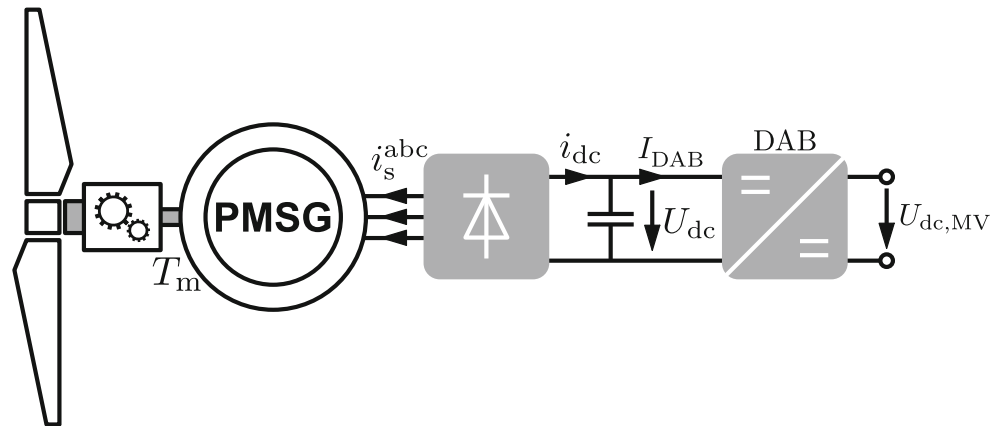
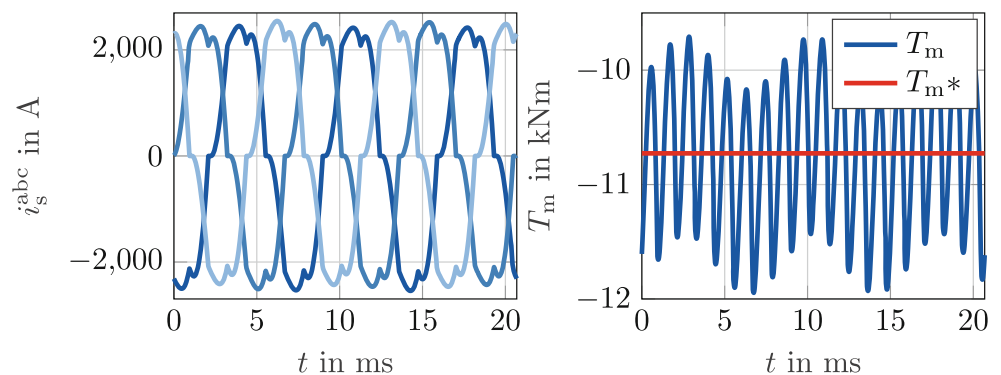


Fig. 10 Plescs simulation of B6-PMG showing stator currents and torque



ical drivetrain have to be investigated further and control strategies for reducing torque ripple should be examined.

3.3 B6-PMG concept

As proposed in [14], a dc-dc boost converter with a three-phase diode rectifier can replace the MSC and thereby reduce switching losses caused by pulse-width modulation (PWM). As the diode rectifier is uncontrolled and therefore cannot excite the generators rotor flux, a PMSG is required. Figure 9 shows the schematic of the novel concept with a DAB3 used as dc-dc boost converter.

The rotor induces a back electromotive force:

$$\hat{U}_{\text{emf}} = p \cdot \Omega_m \cdot \Psi_f$$

in the stator with number of pole pairs p , mechanical rotor speed Ω_m and rotor flux Ψ_f . When the diode rectifier operates in continuous conduction mode, the fundamental component of the stator voltage $|\hat{U}_s|$ is given by:

$$|\hat{U}_s| = \frac{2}{\pi} \cdot U_{\text{dc}}.$$

The resulting voltage drop across the stator reactance X_s generates a current in the stator windings and a resulting torque:

$$T_m = \frac{3}{2} \cdot \frac{|\hat{U}_s| \cdot \hat{U}_{\text{emf}}}{\Omega_m \cdot X_s} \cdot \sin \delta.$$

Hereby, δ is the angle between U_{emf} and \underline{U}_s . Consequently, the dc-dc converter can control the torque by controlling its input voltage U_{dc} . Figure 10 presents results of a PLECS simulation. A PMSG with a rated power of $P_{\text{PMSG}} = 3.3 \text{ MW}$ and rated line-to-line voltage $U_{\text{LL,WT}} = 690 \text{ V}$ is turning at nominal speed. The DAB3 operates with a switching frequency of $f_{\text{sw}} = 1 \text{ kHz}$ steps up its input voltage U_{dc} to the cable voltage $U_{\text{dc,MV}} = 5 \text{ kV}$. Similar to the DC-DFIG, the diode rectifier causes additional harmonics in the stator currents and accordingly in the resulting torque. As the dc link voltage must decrease with increasing torque and the dc link current increases at the same time, it should be investigated how a DAB3 needs to be designed for this application.

4 Analysis

This section evaluates a WT coupled to an electrolyzer and compares each of the presented dc concepts with existing ac concepts. At first, the calculation of investment cost and loss energy is presented.

4.1 Investment cost and operating cost

The cost for power electronic converters decrease since decades because of mass production and increasing amount of RES [15]. Therefore, investment cost are assumed to be 20 €/kVA for a 2L-AFE [5]. For a diode rectifier, investment cost are estimated to be 5 €/kVA based on the market price of an Infineon DN4201 diode [16]. Investment cost for a filter are estimated to be 5 €/kVA based on market prices for a Schaffner FN5060HV output filter. This filter component is suitable for this application because it has a nominal voltage of 690 V and rated current of 1200 A [17]. Investment cost of a 50 Hz transformer are estimated according to [15] under consideration of current prices for copper ($p_{\text{Cu}} = 8000 \text{ €/t}$) and steel ($p_{\text{Fe}} = 600 \text{ €/t}$) as approximately 30 €/kVA . Although the manufacturing of a medium-frequency transformer requires significantly less material, it has not yet been produced in large quantities. Based on estimates from the Institute for Power Generation and Storage Systems, the cost of an medium-frequency transformer is therefore 20 €/kVA . Since a DAB3 consists of two 2L-AFE and a medium-frequency transformer, its investment cost are assumed as 60 €/kVA . For the cable cost, the required conduction material, copper, is considered here. With the previously mentioned copper price p_{Cu} and a peak current density of 1.6 A/mm^2 , cable cost are calculated as:

$$C_{\text{cable,ac}} = 3 \cdot \rho_{\text{Cu}} \cdot p_{\text{Cu}} \cdot A_{\text{cable,ac}} \cdot l_{\text{cable}}$$

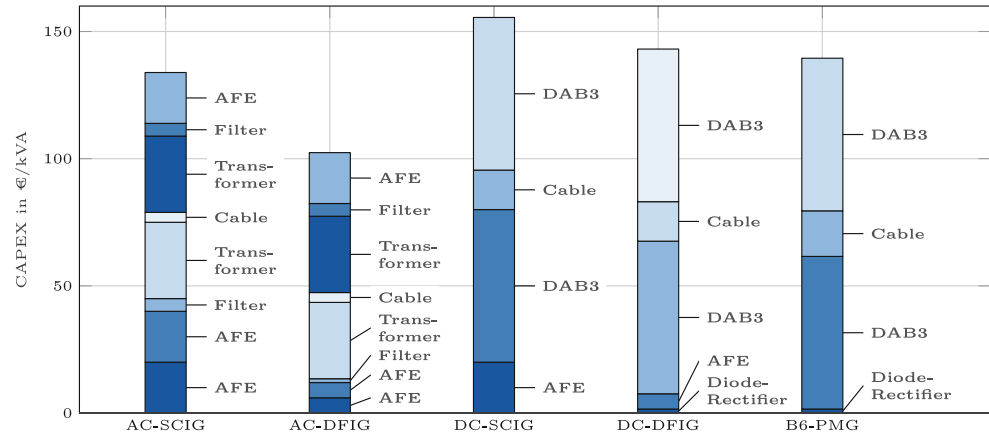
for an ac cable with cross-section area $A_{\text{cable,ac}}$ and:

$$C_{\text{cable,dc}} = 2 \cdot \rho_{\text{Cu}} \cdot p_{\text{Cu}} \cdot A_{\text{cable,dc}} \cdot l_{\text{cable}}$$

for a dc cable with cross-section area $A_{\text{cable,dc}}$. Hereby, the specific copper mass is given by ρ_{Cu} and the cable length by l_{cable} .

For determining the annual operation cost due to energy loss, the efficiency of power electronic converters, transformers and cables are considered as constant over all operation points. Other costs, for example maintenance cost, are neglected. For a 2L-AFE an efficiency of 98% is assumed [18]. According to data sheet values of an Infineon DN4201 diode, the efficiency of a diode rectifier is estimated as 99.5% . Based on the typical losses provided in the data sheet of the Schaffner FN5060HV output filter [17], efficiency of the filter is assumed to be 99.8% . As the DAB3 is a highly efficient converter, its efficiency reaches values even beyond 99% [19]. Here, efficiency of a DAB3 is assumed to be 99% . The efficiency of a 50 Hz transformer

Fig. 11 CAPEX comparison of different ac and dc configurations



is also assumed to be 99%. Then, the annual operating cost for each component is given by:

$$C_{\text{loss}} = p_{\text{energy}} \cdot E_{\text{loss}}.$$

It is assumed that the E_{loss} could have been compensated with $p_{\text{energy}} = 8.4 \text{ ct/kWh}$ [20].

The economic feasibility of different WT concepts is evaluated by calculating the net present value (NPV) according to Eq. 1. This allows to compare total expenditures over lifetime a in years.

$$NPV = C_{\text{inv}} + \sum_{t=1}^a \frac{C_{\text{loss}}}{(1+i)^t} \quad (1)$$

with interest rate i .

It is important to mention that the introduced calculations do not include all investment cost which have to be covered. Investment cost for generator, tower, nacelle, rotor blades and also the electrolyzer are not considered because they are similar for ac and dc concepts. Consequently, the results cannot be used for general investment decisions regarding onshore wind parks. However, this analysis can be used to

assess the costs of coupling wind energy and electrolysis either via ac technology or dc technology.

4.2 Economic evaluation

Within this analysis, an exemplary WT is considered for 5 different concepts: ac full-scale (AC-SCIG), ac partial-scale (AC-DFIG), dc full-scale (DC-SCIG), dc partial-scale (DC-DFIG) and B6-PMG. In each configuration, the WT is coupled to an electrolyzer via a cable with length $l_{\text{cable}} = 1 \text{ km}$. Figure 11 depicts the estimated investment cost for each concept in a bar chart. The individual segments of each bar correspond to the contributions of the respective components, as required according to Figs. 3 and 4.

It can be seen that the initial investment cost is lower for both ac concepts. Although two grid side inverters are omitted in the dc concept, replacing a 50Hz transformer with a DAB3 increases initial investment cost. This is due to the fact that each DAB3 consists of two 2L-AFE and a medium-frequency transformer. In addition to that, the cable costs are higher in the dc concept as the nominal voltage is reduced. The partial-scale concept is less cost-intensive compared to the full-scale concept for ac and dc, because the MSC is only rated for 30% of the nominal

Fig. 12 Loss comparison of different ac and dc configurations

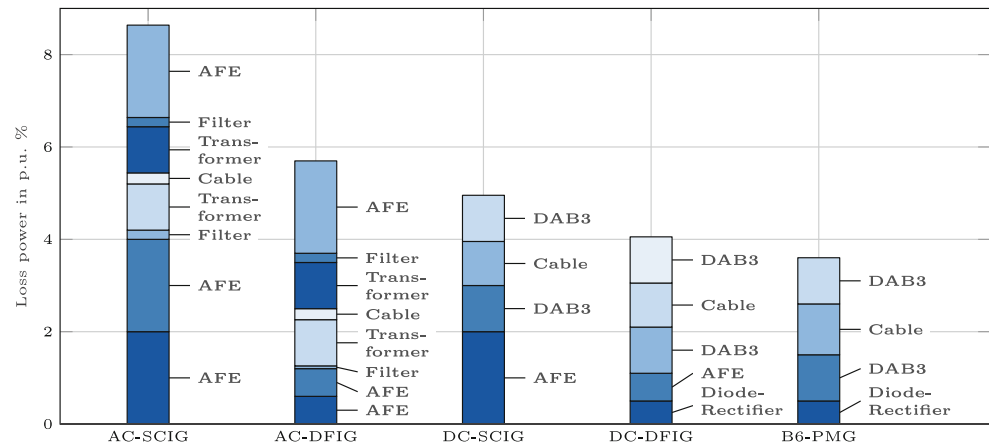
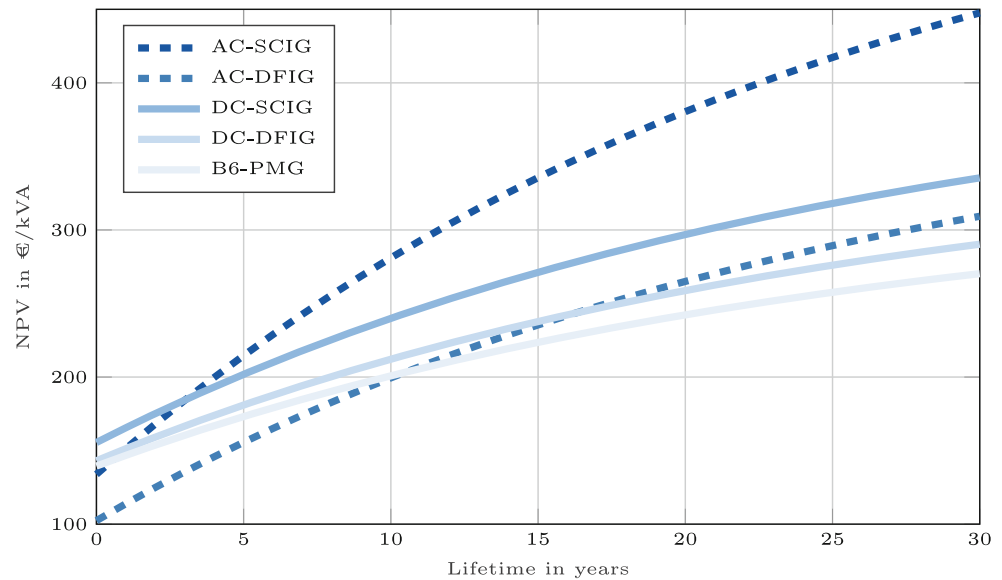


Fig. 13 NPV comparison of different ac and dc configurations



system power. The B6-PMG utilizes a diode rectifier as an MSC and therefore requires the smallest initial investment of the dc concepts.

To evaluate the efficiency, Fig. 12 shows the contribution of every component to the total losses in each concept during nominal operation in a bar chart.

Compared to the ac concepts, the total losses of the dc concepts are lower, whereby the partial-power concepts each have lower losses than the full-power concepts. The former can be explained by the fact that a large part of the power loss is accounted for by the 2L-AFE, of which there are fewer in the ac concepts. The power loss is also lower for inverters of the partial-power concepts. The lowest power loss occurs with the B6-PMG concept, as no 2L-AFE is used as an MSC here. However, the cable losses are higher within the dc concepts because they are operated with a nominal voltage of 5 kV, while the ac cables have a nominal voltage of 20 kV.

As previously observed, the initial investment cost of the ac concepts are lower while the dc concepts cause lower energy losses during operation. In order to put these different trends in relation to each other, Fig. 13 visualizes the NPV for each concept dependent on the system's lifetime.

Calculation of the NPV was done using Eq. 1 assuming annual full-load hours of 2500h and an interest rate of 4%. Under the given parameters, the initially increased investment cost of the dc concepts are compensated due to a higher overall system efficiency after 1–16 years. Full-scale (ac) requires the highest NPV of investment due to both relatively high initial investment and energy loss. In

contrast, partial-scale (dc) and B6-PMG are able to compensate a higher initial investment compared to partial-scale (ac) after approximately 11 and 16 years and require the lowest NPV of investment. Moreover, the full-scale (dc) concept is not able to fall below partial-scale (ac) under the given parameters.

5 Conclusion

In this work, three different dc wind turbine concepts for coupling a WT with an electrolysis system are presented and evaluated in comparison with existing solutions. A full-scale concept and a partial-scale concept are derived from existing ac concepts and a new concept based on a high power dc-dc converter is introduced. Although the dc concepts require higher initial investment cost, the higher system efficiency compensates for this over lifetime. The higher efficiency of the dc systems is achieved through a lower number of conversion stages as the grid-tied converters are no longer required. With the partial-scale concept and the new B6-PMG concept, it is important to examine the effects on the WT's mechanical drivetrain more closely. The diode rectifier connected to the stator introduces additional current harmonics. These harmonics, in turn, lead to increased torque ripple.

Funding Open Access funding enabled and organized by Projekt DEAL.

Open Access Dieser Artikel wird unter der Creative Commons Namensnennung 4.0 International Lizenz veröffentlicht, welche die Nutzung, Vervielfältigung, Bearbeitung, Verbreitung und Wiedergabe in jeglichem Medium und Format erlaubt, sofern Sie den/die ursprünglichen Autor(en) und die Quelle ordnungsgemäß nennen, einen Link zur Creative Commons Lizenz beifügen und angeben, ob

Änderungen vorgenommen wurden. Die in diesem Artikel enthaltenen Bilder und sonstiges Drittmaterial unterliegen ebenfalls der genannten Creative Commons Lizenz, sofern sich aus der Abbildungslegende nichts anderes ergibt. Sofern das betreffende Material nicht unter der genannten Creative Commons Lizenz steht und die betreffende Handlung nicht nach gesetzlichen Vorschriften erlaubt ist, ist für die oben aufgeführten Weiterverwendungen des Materials die Einwilligung des jeweiligen Rechteinhabers einzuholen. Weitere Details zur Lizenz entnehmen Sie bitte der Lizenzinformation auf <http://creativecommons.org/licenses/by/4.0/deed.de>.

References

1. IEA (2023) Global hydrogen review 2023
2. Bühler L, Möst HSD (2023) Grüner wasserstoff: Wie steht es um die wirtschaftlichkeit und welche nachfrage lässt sich erwarten? ifo Institut für wirtschaftsforschung. Niederlassung Dresden, Dresden
3. Statista (2024) Anzahl der wind-volllaststunden nach typischen standorten für windenergieanlagen in deutschland im jahr 2024. <https://de.statista.com/statistik/daten/studie/224720/umfrage/wind-volllaststunden-nach-standorten-fuer-wea/>. Accessed 9 Aug 2024
4. ISE, F.-I.S.E (2024) Öffentliche nettostromerzeugung in deutschland. Energy-Charts
5. Stieneker M (2017) Analyse von mittelspannungsgleichstromnetzen in offshore-Windparks <https://doi.org/10.18154/RWTH-2017-04667>
6. De Doncker RW, Divan DM, Kheraluwala MH A three-phase soft-switched high power density dc/dc converter for high power applications. In: Conference record of the 1988 IEEE industry applications society annual meeting <https://doi.org/10.1109/ias.1988.25153>
7. Stieneker M, Mortimer BJ, Averous NR, Stagge H, De Doncker RW (2014) Optimum design of medium-voltage dc collector grids depending on the offshore-wind-park power. In: IEEE symposium on power electronics and machines for wind and water applications <https://doi.org/10.1109/pemwa.2014.6912218>
8. Hu J, Cui S, De Doncker RW (2018) Dc fault ride-through of a three-phase dual-active bridge converter for dc grids. In: International power electronics conference (IPEC-Niigata 2018—ECCE asia) <https://doi.org/10.23919/ipec.2018.8507672>
9. Nabae A, Takahashi I, Akagi H (1981) A new neutral-point-clamped pwm inverter. IEEE Trans on Ind Applicat. <https://doi.org/10.1109/tia.1981.4503992>
10. Muller S, Deicke M, De Doncker RW (2002) Doubly fed induction generator systems for wind turbines. IEEE Ind Appl Mag. <https://doi.org/10.1109/2943.999610>
11. Wu C, Cheng P, Ye Y, Blaabjerg F (2020) A unified power control method for standalone and grid-connected dfig-dc system. IEEE Trans Power Electron. <https://doi.org/10.1109/tpe.2020.2996267>
12. Nian H, Wu C, Cheng P (2017) Direct resonant control strategy for torque ripple mitigation of dfig connected to dc link through diode rectifier on stator. IEEE Trans Power Electron. <https://doi.org/10.1109/tpe.2016.2630710>
13. Iacchetti MF, Marques GD, Perini R (2015) Torque ripple reduction in a dfig-dc system by resonant current controllers. IEEE Trans Power Electron. <https://doi.org/10.1109/tpe.2014.2360211>
14. Wu B, Kouro S, Lang Y, Zargari N (2011) Power conversion and control of wind energy systems. In: Chapter 9.5: DC/DC boost converter interfaced SG wind energy systems
15. De Doncker RW (2014) Power electronic technologies for flexible dc distribution grids. In: International power electronics conference (IPEC-hiroshima 2014—ECCE ASIA) <https://doi.org/10.1109/ipec.2014.6869670>
16. Infineon (2024) Rectifier diode dn4201n. Documentation
17. Schaffner (2024) Output filter fn5060hv for motor drives. Documentation
18. Song Z, Weidinger P, Zweifel M, Dubowik A (2023) Traceable efficiency determination of a 2.75 mw nacelle on a test bench. Forsch Ingenieurwes. <https://doi.org/10.1007/s10010-023-00650-1>
19. Stieneker M, Averous NR, Soltan N, Stagge H, De Doncker RW (2014) Analysis of wind turbines connected to medium-voltage dc grids. In: 16th European conference on power electronics and applications <https://doi.org/10.1109/epe.2014.6911015>
20. Statista (2020) Durchschnittliche eeg-vergütung von onshore-windenergieanlagen in den jahren 2000 bis 2022 (in euro-cent pro kilowattstunde). <https://de.statista.com/statistik/daten/studie/173266/umfrage/durchschnittliche-eeg-verguetung-von-wind-onshore-bis-2015/>

Publisher's Note Springer Nature remains neutral with regard to jurisdictional claims in published maps and institutional affiliations.